CHIN. PHYS. LETT. Vol. 36, No. 12 (2019) 120601

Observation of $^1S_0 \rightarrow {}^3P_0$ Transition of a $^{40}Ca^+$-$^{27}Al^+$ Quantum Logic Clock *

Si-Jia Chao(晁思嘉)[1,2,3], Kai-Feng Cui(崔凯枫)[1,2], Shao-Mao Wang(汪绍茂)[1,2,3], Jian Cao(曹健)[1,2**], Hua-Lin Shu(舒华林)[1,2**], Xue-Ren Huang(黄学人)[1,2**]

[1] *State Key Laboratory of Magnetic Resonance and Atomic and Molecular Physics, Wuhan Institute of Physics and Mathematics, Chinese Academy of Sciences, Wuhan 430071*

[2] *Key Laboratory of Atom Frequency Standards, Wuhan Institute of Physics and Mathematics, Chinese Academy of Sciences, Wuhan 430071*

[3] *University of Chinese Academy of Sciences, Beijing 100049*

(Received 9 September 2019)

We report the realization of quantum logic spectroscopy on the $^1S_0 \rightarrow {}^3P_0$ clock transition of a single $^{27}Al^+$ ion. This ion is trapped together with a $^{40}Ca^+$ ion in a linear Paul trap, coupled by Coulomb repulsion, which provides sympathetic Doppler laser cooling and also the means for internal state detection of the clock state of the $^{27}Al^+$ ion. A repetitive quantum nondemolition measurement is performed to improve the fidelity of state detection. These techniques are applied to obtain clock spectroscopy at approximately 45 Hz. We also perform the preliminary locking on the $^1S_0 \rightarrow {}^3P_0$ clock transition. Our work is a fundamental step that is necessary toward obtaining an ultra-precision quantum logic clock based on $^{40}Ca^+$-$^{27}Al^+$ ions.

PACS: 06.30.Ft, 32.30.Jc, 37.10.Jk DOI: 10.1088/0256-307X/36/12/120601

With excellent progress in stability and accuracy, optical atomic clocks provide not only a more precise frequency standard but also cutting-edge science research opportunities, such as measuring of fundamental constant variations,[1,2] searching for dark matter,[3] detecting gravitational waves,[4] and clock-based geodesy.[5] Optical clocks based on narrow optical transitions have demonstrated fractional uncertainties with small coefficients approximately 10^{-18} or even 10^{-19} levels,[6–10] surpassing the cesium (Cs) primary frequency standard as the definition of a second of the international system of units (SI).

The $^1S_0 \rightarrow {}^3P_0$ clock transition in $^{27}Al^+$ ion has been recognized as a good candidate[11,12] as an optical frequency reference thanks to its narrow natural linewidth of 8 mHz, its insensitivity to magnetic fields and electric field gradients. In addition, the blackbody radiation shift[13] has a small contribution to the fractional frequency uncertainty level at room temperature (300 K). However, the lack of a laser at 167 nm brings difficulties related to direct laser cooling and detection of $^{27}Al^+$ ion.

Quantum logic spectroscopy (QLS)[14,15] was proposed to overcome these difficulties, which needs an auxiliary ion as the logic ion with multiple choices, such as Be^+ ion,[16] Mg^+ ion,[17–19] or Ca^+ ion.[20–22] The logic ion provides sympathetic cooling, state initialization, and state detection. The internal state of the logic ion is mapped coherently to the internal state of the $^{27}Al^+$ ion via the external vibrational state. As a prerequisite for QLS, the ion pair should be prepared down to the vibrational ground state using sympathetic sideband cooling.

With the development of related technologies, the implementation of optical clocks based on $^{27}Al^+$ ion and $^{25}Mg^+$ ion at the National Institute of Standards and Technology (NIST) have achieved systematic uncertainties at the 10^{-19} level,[10] which introduced advanced technology for the study of the $^{27}Al^+$ ion optical frequency standard. However, we choose the $^{40}Ca^+$ ion as the logic ion in our experiment. Using $^{40}Ca^+$ could minimize the temperature after Doppler cooling during the sympathetic cooling.[23] As the coolant ion, all of the required lasers using $^{40}Ca^+$ for cooling and detection are based on the semiconductor laser, which is easy to obtain.[24] In addition, $^{40}Ca^+$ as a probe ion with higher relative sensitivities can be used to analyze the electromagnetic field of $^{27}Al^+$ in the environment. In the same trap, measurement of the field-induced shifts using the transition frequency of $^{40}Ca^+$ provides more convenience and greater accuracy than $^{27}Al^+$.[25]

In this Letter, we report the realization of QLS on the $^1S_0 \rightarrow {}^3P_0$ clock transition in a single $^{27}Al^+$ ion. A $^{40}Ca^+$-$^{27}Al^+$ pair is trapped in a linear Paul trap, coupled by their Coulomb repulsion. Here, we obtain the spectroscopy of clock transition at approximately 45 Hz using the QLS and repetitive quantum nondemolition (QND) measurement. We also demonstrate preliminary locking on the clock transition. This work represents an important step towards an $^{27}Al^+$ ion quantum logic clock with high precision.

The experimental apparatus used in our experiment is roughly the same as that used in our previous experiment.[22,25] A single $^{40}Ca^+$ ion and a single $^{27}Al^+$ ion are co-trapped in a linear Paul trap,

*Supported by the National Key R&D Program of China under Grant No 2017YFA0304401, the Strategic Priority Research Program of the Chinese Academy of Sciences under Grant No XDB21030100, and the Technical Innovation Program of Hubei Province under Grant No 2018AAA045.

**Corresponding authors. Email: caojian@wipm.ac.cn; shl@wipm.ac.cn; hxueren@wipm.ac.cn

© 2019 Chinese Physical Society and IOP Publishing Ltd

which includes four blade electrodes and two end-cap electrodes. They are all placed in a vacuum chamber with a pressure at approximately 10^{-9} Pa. The trap is driven by a helical resonator at approximately 19.7 MHz with Q-factor of 180. Three pairs of magnetic coils are designed to control the magnetic field at 3.4 G. The direction of magnetic field beyond that is displayed in Fig. 1(a). In addition, a separate coil is set on the direction of magnetic field used to compensate for 50 Hz electric noise from the power supply, and thus the coherence time is prolonged from 64 μs to 383 μs.

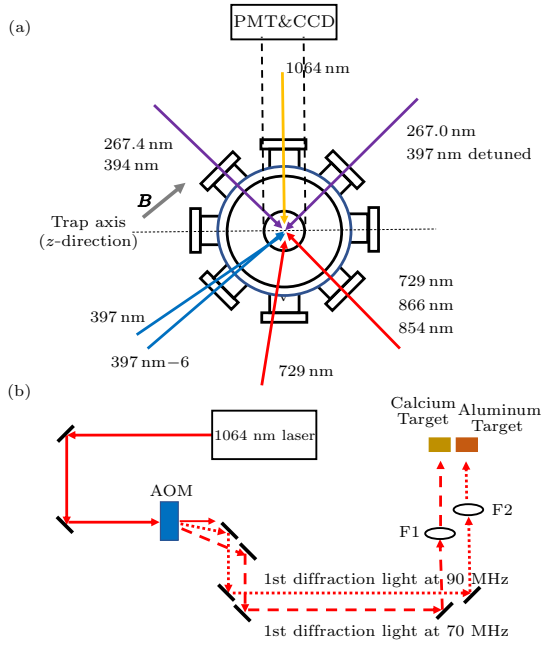

Fig. 1. (a) Top view of the laser path arrangement. The 729 nm laser along the vertical direction are not shown. ***B*** stands for the direction of magnetic field. (b) The optical path of laser ablation. A pulsed laser at 1064 nm is controlled using an AOM. Only the first order of the AOM's diffracted light is used, which is set to 70 MHz for the calcium target and 90 MHz for the aluminum target. F1 and F2 are focusing lenses.

The top view of the laser path arrangement is depicted in Fig. 1(a). The cooling beam, repump beam, prob beam, ionization beam, ablation beam, and clock beam are settled in the horizontal plane. To provide the detection capability of micro-motion in three dimensions, we set up one 729 nm laser in the vertical direction and two lasers in the horizontal direction. The laser beam at 267.0 nm drives the $(^1S_0, F = 5/2) \rightarrow (^3P_1, F = 7/2)$ transition in the $^{27}Al^+$ ion, and another frequency-quadrupled laser beam at 267.4 nm, with approximately 6 Hz linewidth, is used to excite the $^1S_0 \rightarrow {}^3P_0$ clock transition. A photomultiplier tube (PMT) and an electron-multiplying CCD (EMCCD) are employed to collect fluorescence signals using a 5:5 beam splitter.

As shown in Fig. 1(b), the ion pairs are loaded by laser ablation from a metal target. Two targets are placed on a horizontal plane of the trap. A pulsed laser at 1064 nm acts as the ablation laser, which is controlled by an acousto-optic modulator (AOM), and only the first order of the AOM's diffracted light is used. The functions of the AOM are mainly reflected in the following areas: to turn the laser on or off, to adjust the intensity of the laser and to change the position of the laser from the target. To load a $^{40}Ca^+$ ion, the laser is controlled by the AOM, which is set to 70 MHz with a minimum pulse energy of 43 μJ and a pulse duration of 10 ms. It is worth mentioning that the laser intensity is strong enough to obtain the $^{40}Ca^+$ ion directly without the ionization laser in one minute. Generally, a $^{40}Ca^+$ ion lasts for several days without any laser. However, a diode laser at 394 nm is necessary to generate the $^{27}Al^+$ ion. When the AOM is set to 90 MHz, the aluminum atoms are produced using the ablation laser with a minimum pulse energy of 49 μJ and a pulse duration of 10 ms. With the ionization laser, $^{27}Al^+$ can be observed on the EMCCD in 5–8 min.

After loading the ion pair, we performed motional sideband spectroscopy on a $^{40}Ca^+$-$^{27}Al^+$ ion chain consisting of the center-of-mass mode (COM) and breathing mode (BM). After the sympathetic cooling of the $^{27}Al^+$ ion via the $^{40}Ca^+$ ion, both axial modes of the $^{40}Ca^+$-$^{27}Al^+$ pair are cooled simultaneously to near the motional ground state. Comparing the sideband heights yields an average phonon number of 0.052(9) for COM and 0.035(6) for BM,[25] which provides the prerequisites for the interrogation of the clock transition.

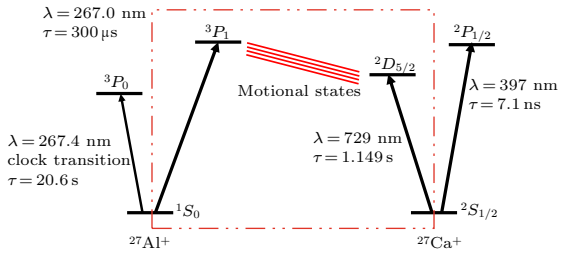

Fig. 2. Transfer of the $^{27}Al^+$ ion clock state to $^{40}Ca^+$ ion for detection. A $^{40}Ca^+$-$^{27}Al^+$ pair is coupled by their Coulomb repulsion. The clock transition of the $^{27}Al^+$ ion is $^1S_0 \rightarrow {}^3P_0$ at 267.4 nm.

Figure 2 shows the transfer of the $^{27}Al^+$ ion clock state to that of $^{40}Ca^+$ ion for detection via $^1S_0 \rightarrow {}^3P_1$ motional-sideband excitation. The typical process of the clock interrogation may be described as follows.[15,16] First, a $^{27}Al^+$ ion is prepared with specific polarization and angular momentum states. Then, the $^{27}Al^+$ ion is interrogated by changing their internal states with a correct probing frequency. When the $^{27}Al^+$ ion is on the $|{\downarrow}{>}_{Al}$, blue sideband (BSB) π-pulse of the $^1S_0 \rightarrow {}^3P_1$ transition on the $^{27}Al^+$ ion will increase one phonon number of the $^{40}Ca^+$-$^{27}Al^+$ pair. Then, red sideband (RSB) π-pulse of the $^2S_{1/2} \rightarrow {}^2D_{5/2}$ transition on the $^{40}Ca^+$ ion will transfer the internal state from $|{\downarrow}{>}_{Ca}$ to $|{\uparrow}{>}_{Ca}$. Finally, the clock state is detected via a $^{40}Ca^+$ ion with

a transition of the $^2S_{1/2} \rightarrow {}^2P_{1/2}$.

When the $^{27}Al^+$ ion is in the $^3P_0$ state after optical pumping, the transfer via the $^1S_0 \rightarrow {}^3P_1$ motional-sideband excitation is blocked, which means that the $^{40}Ca^+$ ion is in the ground state. An average of 12 $^{40}Ca^+$-ion photons of wavelength 397 nm will be counted if the $^{27}Al^+$ ion is in the $^3P_0$ state, as depicted in Fig. 3(a), and an average of two photons will be counted if the $^{27}Al^+$ ion is in the $^1S_0$ state, as shown in Fig. 3(b). Here, histograms of photon counts provide the criterion for judging the state using QND measurements.[26] The QND measurement process does not affect the projected states of the primary system. In addition, the fidelity is limited by decoherence and imperfect ground-state cooling in the single detection. Therefore, we repeat the readout sequence 5–10 times to improve the fidelity of the clock state.

The interrogation and detection sequences are depicted in Fig. 3(c). Generally, the following sequence is repeated approximately 5–10 times to achieve state detection: (1) Sympathetic Doppler cooling: under interrogation, we first cool all six normal modes of the $^{40}Ca^+$-$^{27}Al^+$ pair to the Doppler limit by sympathetic Doppler cooling via a $^{40}Ca^+$ ion (500 μs); (2) ground-state cooling of the axial modes of both the center of COM and BM to the vibrational ground states of one pair of ions (6 ms); (3) a 267.0 nm BSB π-pulse on the $^{27}Al^+$ ion $(^1S_0, F = 5/2) \rightarrow (^3P_1, F = 7/2)$ (15 μs); (4) a 729 nm RSB π-pulse on the $^{40}Ca^+$ ion $(^1S_{1/2}, F = -1/2) \rightarrow (^2D_{5/2}, F = -5/2)$ (25 μs); (5) detection via a $^{40}Ca^+$ ion with 397 nm laser and continuation for about 2–3 ms.

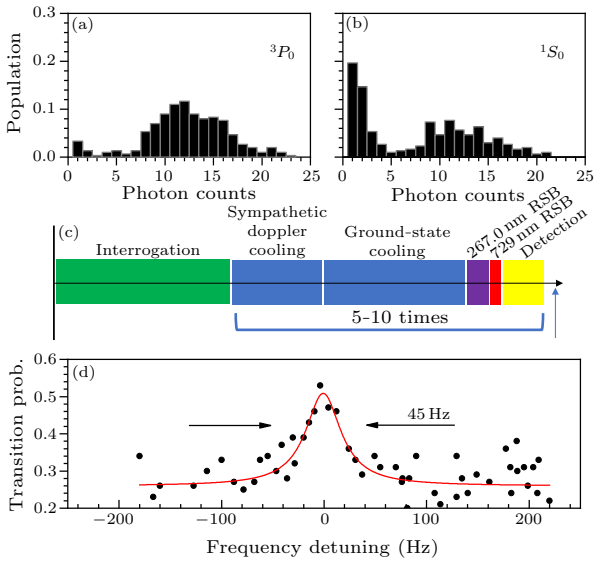

Fig. 3. Histograms of photon counts used for judging (a) $^3P_0$ and (b) $^1S_0$ states in $^{27}Al^+$ ion via fluorescence of $^{40}Ca^+$ ion. (c) Timing sequence for the $^1S_0 \rightarrow {}^3P_0$ clock transition spectrum by the QLS method in $^{27}Al^+$ ions. (d) Clock transition in $^{27}Al^+$ ion based on QLS. The black dots are the experimental data, and the red smooth line is the Lorentzian fit to these data, giving a linewidth of 45 Hz for an interrogation time of 25 ms.

During the detection sequence, it is noticed that the $^3P_1$ excitations usually decay to the $^1S_0$ state on account of the 300 μs lifetime, but the $^3P_0$ excitations do not change with the 20.6 s lifetime. In addition, the ions occasionally collide with the background gas, causing a dark 'cloud' state.[25] In this case, a 397 nm cooling laser that was red detuned at about −150 MHz and the decrease in the trap frequency causes the ions to re-crystallize, while the sequence enters the standby state.

The photon counts are recorded and calculated using a computer, to determine whether the $^{27}Al^+$ ions are in the $^1S_0$ or $^3P_0$ state through a maximum-likelihood analysis. The success of the transition entirely depends on the judgment by the computer, and the readout errors are calculated continuously until the error decreases below 5%. With this method, the clock spectroscopy with a linewidth of 45 Hz is obtained with a 25 ms interrogation time across the $^1S_0 \rightarrow {}^3P_0$ resonance, as shown in Fig. 3(d). Theoretically, longer interrogation times are better for narrower clock spectra. Moreover, the achievable linewidth in clock spectroscopy is limited by various factors, including coherence between the laser and ions. As can be seen from the diagram in Fig. 3(d), the results have obvious background noise and unsatisfactory fidelity mainly because of the decoherence. For an implementation of quantum operation, a coherence time much longer than the operation time is a better condition.[27] Using contrast of the Ramsey pattern can assess the decoherence of motional superpositions, the coherence time is about 383 μs, which is barely enough for quantum logic operations. The decoherence issue not only leads to linewidth enhancement but also brings a height reduction of the spectral line, which is mainly from the external magnetic field as a result of the magnetic sensitivity of the $^{40}Ca^+$ ion.

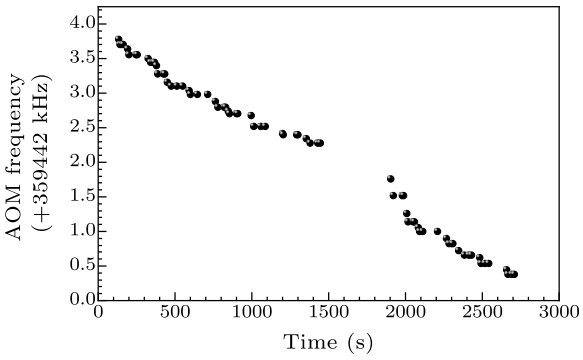

Fig. 4. The drift of the $^1S_0 \rightarrow {}^3P_0$ clock transition frequency based on the AOM. The black dots are the experimental data for nearly 50 min. The gap indicates that the aluminum ion reacted with the background hydrogen to form aluminum hydride ions, which implies the need to reload the $^{40}Ca^+$-$^{27}Al^+$ pair.

In Fig. 4, the preliminary locking of the $^1S_0 \rightarrow {}^3P_0$ clock transition uses two points locked on a single peak, which is mainly influenced by the drift of the clock transition laser. Subject to that the clock tran-

sition laser has a frequency drift about 500 kHz per day, we selected a single peak of linewidth 6 kHz over a duration of nearly 50 min. The reason for the gap in the data (about 500 s) is attributed to the need to reload the $^{40}Ca^{+}$-$^{27}Al^{+}$ pair. Under ultrahigh vacuum conditions, because a combination reaction could occur between the $^{27}Al^{+}$ ion and the background gas, a pair of ions usually lasts for several minutes during the detection of clock transition. In reality, an ion pair storage time is an obstacle to long duration locking, which is influenced by the degree of vacuum in the system.

In summary, we have demonstrated an experimental study and results on observing the spectroscopy of the $^{1}S_0 \rightarrow {}^{3}P_0$ clock transition in $^{27}Al^{+}$ using $^{40}Ca^{+}$ as the auxiliary ion. We have also realized a preliminary locking for the clock transition. There are still some drawbacks that need to be improved for closed-loop operation of the $^{40}Ca^{+}$-$^{27}Al^{+}$ quantum logic clock, such as low fidelity, and short lifetimes of ions, compared to others. One reason for this may be the decoherence of the magnetic field, which can be improved by compensation of magnetic fields to promote coherent time. Moreover, to increase the lifetimes of the ions, a renovated system with higher vacuum is needed and pure titanium material is necessary. In addition, further optimization for sympathetic ground-state cooling by means of cooling with not only the axial motional modes but also the radial motional modes to the ground states is needed. With these improvements, we expect to further narrow the clock spectrum and realize long duration locking operation of the clock.

We thank for D. Hume, A. Hankin for their fruitful discussion.

References

[1] Huntemann N, Lipphardt B, Tamm Chr, Gerginov V, Weyers S and Peik E 2014 *Phys. Rev. Lett.* **113** 210802
[2] Blatt S, Ludlow A D, Campbell G K, Thomsen J W, Zelevinsky T, Boyd M M, Ye J, Baillard X, Fouché M and Le Targat R et al 2008 *Phys. Rev. Lett.* **100** 140801
[3] Derevianko A and Pospelov M 2014 *Nat. Phys.* **10** 933
[4] Kolkowitz S, Pikovski I, Langellier N, Lukin M D, Walsworth R L and Ye J 2016 *Phys. Rev. D* **94** 124043
[5] Chou C W, Hume D B, Rosenband T and Wineland D J 2010 *Science* **329** 1630
[6] Campbell S L, Hutson R B, Marti G E, Goban A, Oppong N D, McNally R L, Sonderhouse L, Robinson J M, Zhang W, Bloom B J et al 2017 *Science* **358** 90
[7] McGrew W F, Zhang X, Fasano R J, Schäffer S A, Beloy K, Nicolodi D, Brown R C, Hinkley N, Milani G, Schioppo M et al 2018 *Nature* **564** 87
[8] Keller J, Burgermeister T, Kalincev D, Didier A, Kulosa A P, Nordmann T, Kiethe J and Mehlstäubler T E 2019 *Phys. Rev. A* **99** 013405
[9] Huntemann N, Sanner C, Lipphardt B et al 2016 *Phys. Rev. Lett.* **116** 063001
[10] Brewer S M, Chen J S, Hankin A M, Clements E R, Chou C W, Wineland D J, Hume D B and Leibrandt D R 2019 *Phys. Rev. Lett.* **123** 033201
[11] Dehmelt H G 1982 *IEEE Trans. Instrum. Meas.* **IM-31** 83
[12] Yu N, Dehmelt H and Nagourney W 1992 *Proc. Natl. Acad. Sci. USA* **89** 7289
[13] Safronova M S, Kozlov M G and Clark C W 2011 *Phys. Rev. Lett.* **107** 143006
[14] Wineland D J, Bergquist J C, Bollinger J J, Drullinger R E and Itano W M 2002 *World Scientific* **361**
[15] Schmidt P O, Rosenband T, Langer C, Itano W M, Bergquist J C and Wineland D J 2005 *Science* **309** 749
[16] Rosenband T, Schmidt P O, Hume D B, Itano W M, Fortier T M, Stalnaker J E, Kim K, Diddams S A, Koelemeij J, Bergquist J C et al 2007 *Phys. Rev. Lett.* **98** 220801
[17] Chen J S, Brewer S M, Chou C W, Wineland D J, Leibrandt D R, Hume D B 2017 *Phys. Rev. Lett.* **118** 053002
[18] Ksenia K, Ilia Z, Ilya S, Alexander B, Nikolay K 2018 *European Frequency and Time Forum* (Turin, Italy 10–12 April 2018) p 377
[19] Liu H L, Xu Z T, Ma Z Y, Wei W Z, Hao P, Yuan W H, Che H, Cheng F H, Wang Z Y, Deng K et al 2019 arXiv:1902.09716 [physics.atom-ph]
[20] Guggemos M, Heinrich D, Herrera-Sancho O A, Blatt R and Roos C F 2015 *New J. Phys.* **17** 103001
[21] Hannig S, Pelzer L, Scharnhorst N, Kramer J, Stepanova M, Xu Z T, Spethmann N, Leroux I D, Mehlstäubler T E and Schmidt P O 2019 *Rev. Sci. Instrum.* **90** 053204
[22] Shang J J, Cui K F, Cao J, Wang S M, Chao S J, Shu H L and Huang X R 2016 *Chin. Phys. Lett.* **33** 103701
[23] Wübbena J B, Amairi S, Mandel O and Schmidt P O 2012 *Phys. Rev. A* **85** 043412
[24] Cao J, Zhang P, Shang J, Cui K, Yuan J, Chao S, Wang S, Shu H and Huang X 2017 *Appl. Phys. B* **123** 112
[25] Cui K F, Shang J J, Chao S J, Wang S M, Yuan J b, Zhang P, Cao J, Shu H L and Huang X R 2018 *J. Phys. B* **51** 045502
[26] Hume D B, Rosenband T and Wineland D J 2007 *Phys. Rev. Lett.* **99** 120502
[27] Turchette Q A, Kielpinski D, King B E et al 2000 *Phys. Rev. A* **61** 063418